BEAM DIAGNOSTICS FOR CSNS-II LINAC COMMISSIONING AND OPERATION*

J. $Peng^{1,2\dagger}$, Y. L. $Han^{1,2}$, Z. P. $Li^{1,2}$, Y. $Li^{1,2}$, Y. Yuan^{1,2}, X. Y. $Feng^{1,2}$, M. Y. $Huang^{1,2}$, H. C. $Liu^{1,2}$, S. $Wang^{1,2}$, S. N. $Fu^{1,2}$

¹Institute of High Energy Physics, Chinese Academy of Sciences, Beijing, China ²Spallation Neutron Source Science Center, Dongguan, China

Abstract

The China Spallation Neutron Source (CSNS) facility began operation in 2018. By 2020, its accelerator achieved the design power of 100 kW and currently operates at a power of 160 kW. This year, the power upgrade project (CSNS-II) has been launched to meet the growing scientific demands. Our goal is to enhance the accelerator power to 500 kW primarily by increasing the beam current. A comprehensive suite of beam diagnostics has been developed to support commissioning and operation of the accelerator at higher intensities. In this paper, we first review the commissioning and operational status of the existing linac, and then outline the new requirements for the linac upgrade.

INTRODUCTION



Figure 1: Overview of the CSNS-II linac layout.

Table 1: Upgraded Parameters of the CSNS Accelerator

Parameter	Units	CSNS	CSNS-II
Average power	kW	100	500
Beam energy	GeV	1.6	1.6
Peak linac current	mA	15	40
Pulse length	μs	500	650
Pulse repetition	Hz	25	25+25 ¹
frequency			

¹ The 25 Hz beam pules are injected downward into the RCS, while the other 25 Hz pules are directed upward to the experimental stations.

The CSNS accelerator comprises an 80 MeV linac serving as the injector and a 1.6 GeV rapid cycling synchrotron (RCS) [1-2]. The linac includes a 50 keV H- ion source, a 3 MeV RFQ, an 80 MeV DTL, and several beam transport lines. In 2024, the CSNS power upgrade project was launched. The beam power of the accelerator will be increased to 500 kW by raising the beam peak current from 15 mA to 40 mA, as shown in Table 1. To mitigate the space charge effect [3], the linac energy will be upgraded from 80 MeV to 300 MeV by adding a superconducting linac after the DTL. As shown in Fig. 1, the superconducting linac consists of two sections: a

324 MHz spoke section and a 648 MHz elliptical section. With the increase in both current and energy of the linac, the beam transport lines have been completely redesigned, and the diagnostics installed in these lines have also been adjusted accordingly. This paper reviews the beam commissioning status and provides a summary of the changes in diagnostics.

DIAGNOSTICS LAYOUT

LEBT

The Low Energy Beam Transport (LEBT) is equipped with two BCMs to measure the beam current and calculate beam transmission. Additionally, it contains a double-slit emittance monitor designed to measure the transverse phase space distribution of the beam.

MEBT

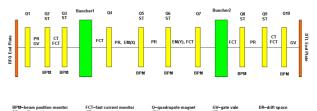


Figure 2: MEBT layout for the CSNS linac.

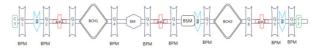


Figure 3: New MEBT scheme for the CSNS-II linac.

The Medium Energy Beam Transport (MEBT) of the CSNS is shown in Fig. 2, and it has been redesigned for the CSNS-II linac, shown in Fig. 3. Comparing to the old MEBT layout the numbers of magnets and bunchers remained unchanged in the new MEBT scheme, so the lengths of two MEBTs are nearly the same. To explore characteristics of high-intensity beam, more diagnostics have been incorporated into the new MEBT scheme. Wire scanners and double-slit emittance monitor have proven useful for determining the phase space of the beam output from the RFQ. The emittance monitor can directly plot the phase space distribution of beam in the middle of the MEBT, as shown in Fig. 4. The Wire scanners can be used to monitor the beam envelope along the MEBT, as shown in Fig. 5. Figure 6 depicts the simulated beam distribution at the location of the emittance monitor by fitting with the measured beam profile. Compared to the results by emit-

^{*} Work supported by 2023YFA1606802, DG24313511

[†] pengjun@ihep.ac.cn

tance monitor, the difference between two groups of ellipse emittance is less than 12% [4].

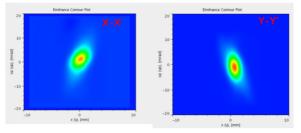


Figure 4: Measured transverse emittance with double-slit emittance monitor in the MEBT.

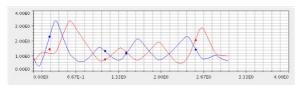


Figure 5: Measured horizontal profile(red) and vertical profile(blue) in the MEBT.

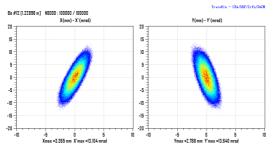


Figure 6: Simulated transverse emittance at the location of emittance monitor fitting with measured beam profiles by wire scanners.

In the new MEBT scheme, eight BPMs are used for beam orbit measurement and beam phase measurement, replacing the originally used FCTs. The purpose of changing from FCTs to BPMs is to provide enough space for transverse collimators. As the beam intensity increasing, various nonlinear effects will be enhanced, leading to more halo particles. To mitigate beam loss in the downstream linac, it is essential to remove halo particles at the low energy section. Therefore, a group of three transverse collimators is placed in the new MEBT, with the capability of removing up to 3% of the full beam power.

During the beam commissioning of the old MEBT, some irregular beams were lost in the DTL tanks, causing sparking. To avoid this issue, we add a Faraday Cup in the new MEBT, to serve as a beam stop during the commissioning of the Front-end and the MEBT.

For the CSNS linac, no diagnostics were originally designed for monitoring beam longitudinal parameters. Lacking longitudinal beam information made it challenging to tune the longitudinal mismatch. Therefore, we add a BSM in the new MEBT to monitor the beam longitudinal profile as it leaves the RFQ.

There are two BCMs at the entrance and exit of the MEBT for current measurement.

DTL

The DTL consists of four tanks with a final output energy of 80 MeV. Each drift tube in the DTL tank contains an electromagnet, and no diagnostics or steering magnets have been installed in the DTL tanks. Only a BPM placed between DTL3 and DTL4 is used to monitor the relative change in beam position.

The distance between the two tanks is designed to be $1\beta\lambda$, which can only accommodate a FCT plus a BCM. The BCMs are used to monitor the beam transmission, while the FCTs are used for measuring the beam phase. The output energy of each tank can be calculated using two downstream FCTs based on the TOF (Time of Flight) method.

For DTL tanks, it is essential to find the correct RF amplitude and phase settings to minimize energy spread and mismatch. A method called "phase scan signature matching" was adopted for determining the RF set points of DTL tanks [5-6]. This method involves varying the RF amplitude and phase settings of a cavity over a fairly large range and comparing the measured downstream beam phase response "signatures" to model predictions, as shown in Fig. 7 [7]. The RF amplitude, relative phase of the beam and the input energy are used as variables in model fitting. After that, the DTL tank can be set at the design amplitude and phase calculated with the calibrated amplitude and phase.

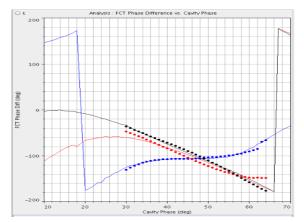


Figure 7: Plots of the DTL tank1 phase scan for nominal RF amplitude (red), 3% below nominal (blue) and 3% above nominal (black).

For the CSNS-II linac, the FCTs placed between the DTL tanks will be replaced with BPMs, which can simultaneously monitor beam orbit.

LEDP

LEDP is a short beam line, 1.86 meters long, that connects the normal conducting linac to the cold linac. The main function of the LEDP is to minimize gas flow into the cold linac. A Faraday Cup is installed at the exit of the LEDP to be used for the commissioning of the normal conducting linac. Besides meeting vacuum requirement, the LEDP also serves as a matching section. It contains

two quadrupoles, two BPMs, a BSM, a wire scanner and a BCM.

Superconducting Linac

The superconducting linac consists of the Spoke section and the Elliptical section, as shown in Fig. 8. Between cryomodules, warm magnet doublets can be used to house the diagnostics. Each warm unit includes one BPM for beam position and phase measurement, which can be used to calibrate the RF amplitude and phase of the superconducting cavity.

In the first four periods of each section, four wire scanners are used to obtain the transverse Twiss parameters and emittance. At the end of each section, a BCM is used to measure the beam current and calculate the beam transmission.

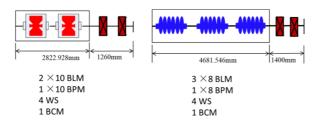


Figure 8: Layout of the spoke period and elliptical period.

LRBT

The Linac to RCS Beam Transport (LRBT) is a long beam transport line designed to transport the beam output from the linac into the RCS. The LRBT consists of nine triplet focusing periods, two matching sections and several bending magnets and quadrupoles to guide the beam for injection into the RCS. In addition to the magnets, it contains a debuncher to tune the beam energy spread to meet the RCS injection requirement.

There are a total of six wire scanners installed in the LRBT. Five of them are used to measure the beam Twiss parameters and emittance of the beam at the exit of the DTL and the last one is used to monitor beam profile before bending downward. Figure 9 shows the measured beam profiles in the LRBT [8-9].

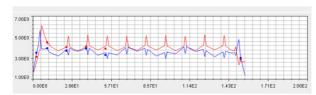


Figure 9: Measured horizontal profile (red) and vertical profile (blue) in the LRBT.

The LRBT is also redesigned for the CSNS-II linac where five triplets are replaced by a superconducting linac. Two debunchers will be installed to tune the beam center jitter and the beam energy spread. The new LRBT contains fourteen BPMs, six wire scanners, three BCMs, three WCMs and one BSM.

CONCLUSION

For the CSNS-II project, the beam energy and current are both upgraded. A superconducting linac will be installed after the DTL, and the beam transport lines between each accelerating section have been redesigned. The diagnostics installed in these beam lines are also changed accordingly. The primary adjustments are replacing FCTs with BPMs, adding longitudinal diagnostics and using Faraday Cups. Those diagnostics testified helpful for beam commissioning of CSNS linac have been preserved.

REFERENCES

- S. Fu et al., "Status of CSNS Project", in Proc. IPAC'13, Shanghai, China, May 2013, paper FRXAB201, pp. 3995-3999.
- [2] S. Wang et al., "Introduction to the overall physics design of CSNS accelerators", Chin. Phys. C, vol. 33, pp. 1-3, 2009. doi:10.1088/1674-1137/33/S2/001
- [3] M.Y. Huang *et al.*, "Performance and upgrade considerations for the CSNS injection", in *Proc. HB2023*, Geneva, Switzerland, 9-13 October 2023, THA111, pp. 326-330. doi:10.18429/JACOW-HB2023-THA111
- [4] J. Peng et al., "Beam Commissioning Results for the CSNS MEBT and DTL-1", in Proc. HB'16, Malmö, Sweden, Jul. 2016, pp. 329-332. doi:10.18429/JACOW-HB2016-TUPM2Y01
- [5] T. L. Owens, M. B. Popovic, "Phase scan signature matching for Linac tuning", Particle Accelerators, 1994, Vol.48, pp.169-179.
- [6] J. Galambos, A. V. Aleksandrov, C. Deibele, and S. Henderson, "PASTA An RF Phase and Amplitude Scan and Tuning Application", in *Proc. PAC'05*, Knoxville, TN, USA, May 2005, paper FPAT016, pp. 1491-1493.
- [7] J. Peng et al., "Beam Commissioning Results of the CSNS Linac", in Proc. IPAC'17, Copenhagen, Denmark, May 2017, pp. 1223-1225.
 - doi:10.18429/JACoW-IPAC2017-TUOBA1
- [8] J. L. Sun *et al.*, "Commissioning of the Beam Instrumentation System of CSNS", in *Proc. IBIC'20*, Santos, Brazil, Sep. 2020, pp. 7-10. doi:10.18429/JACOW-IBIC2020-MOA003
- [9] Z. P. Li, Y. Li, J. Peng, and S. Wang, "Beam Commissioning of Transport Line LRBT of CSNS", in *Proc. IPAC'17*, Copenhagen, Denmark, May 2017, pp. 2314-2316. doi:10.18429/JACOW-IPAC2017-TUPVA098